Review article

Valerie Popp, Philipp Ansorg*, Burkhard Fleck and Cornelius Neumann

Temporal coherence properties of laser modules used in headlamps determined by a Michelson interferometer

https://doi.org/10.1515/aot-2020-0039
Received June 30, 2020; accepted October 29, 2020;
published online November 23, 2020

Abstract: In this work, an investigation of the temporal coherence properties of radiation which is emitted by laser modules integrated in headlamps is presented. The motivation for these measurements was difficulties concerning the field of classification for laser products which function as conventional headlamps. Based on an experimental setup including a Michelson interferometer, a goniophotometer and a spectrometer, coherence lengths of 92.5 and 147.0 μm are obtained for two different laser modules. The results show that the temporal coherence of the examined radiation is appreciably higher than the temporal coherence of conventionally produced white light. Therefore, at this point in time, laser modules used in headlamps cannot be considered as customary white light sources.

Keywords: headlamp; laser; temporal coherence.

1 Introduction

Currently, everyone is faced with the omnipresent technological progress at any time. Of course, also in the field of automotive lighting innovations are generated regularly. They are driven by the desire to increase the road safety, especially at night. After halogen, xenon and LED headlights, the latest development concerns laser headlamps. They offer many advantages, for example a light density which is about five times higher compared to other light source technologies, a compact design, and the potential for innovative functions [1, 2]. The used laser modules produce light with the help of a luminescence conversion. Radiation of blue laser diodes is partly converted into broadband light with longer wavelengths, and the mixture of the scattered remaining blue radiation with the converted radiation leads to white light. Thereby, laser modules are used as conventional lamps. But this resulted in a problem concerning the classification of the headlamps including such modules. Laser products have to be classified under the IEC 60825-1 (Safety of laser products – Part 1: Equipment classification and requirements). Though, this classification system is based on collimated laser beams, and this is not appropriate to classify radiation emitted for lighting by headlamps. Therefore, the application of the IEC 60825-1 to classify laser headlamps led to an over-conservative and strict framework for headlamp manufacturers [3–5]. Such a headlamp would be a Class 3R or 3B laser product, so severe requirements have to be fulfilled, which is very elaborate [3]. However, conventional headlamps as xenon headlights get classified under the IEC 62471 (Photobiological safety of lamps and lamp systems) by allocation of a risk group. To solve this situation, the new subclause 4.4 (Laser products designed to function as conventional lamps) was added to the IEC 60825-1 Ed.3 from 2014. It permits the classification of the accessible emission under the IEC 62471, whereby the product as such still falls within the scope of IEC 60825-1. When no other laser radiation exits the source, this usually leads to a classification of the product as Class 1 laser product. In addition, a certain risk group in accordance with the IEC 62471 is assigned independently of the criteria of the laser classification framework. But, three requirements have to be fulfilled to apply subclause 4.4: The device has to function as a conventional lamp, it has to exhibit a certain minimum angular subtense, and the maximum radiance must not exceed a specific value.

Actually, some countries did not yet accept the third edition from 2014 of the IEC 60825-1 but rather the second

***Corresponding author: Philipp Ansorg**, Entwicklung Funktionen Licht, AUDI AG, Ingolstadt, Germany, E-mail: philipp.ansorg@audi.de
Valerie Popp, Entwicklung Innovationen Licht/Sicht, AUDI AG, Ingolstadt, Germany, E-mail: valerie.graf@gmail.com
Burkhard Fleck, SciTec – Präzision-Optik-Materialien, Ernst-Abbe-Hochschule Jena, Jena, Germany, E-mail: burkhard.fleck@eah-jena.de
Cornelius Neumann, Lichttechnisches Institut, Karlsruher Institut für Technologie, Karlsruhe, Germany,
E-mail: cornelius.neumann@kit.edu

edition from 2007 which does not include the subclause 4.4. For car manufacturers, this leads to the problem of classification and labelling of the product. Therefore, for discussions with legal authorities or custom offices, this work tries to give another argument why the emitted radiation of a laser-sourced headlamp has no typical laser characteristic regarding the temporal coherence and should be treated as a product of laser class 1. By measuring the property of temporal coherence of laser headlamps and compare it with laser sources and lamp systems, the headlamp is tried to be classified as one of these.

Therefore, the aim of this paper is the investigation of the temporal coherence properties of radiation which is emitted by laser modules integrated in headlamps and the comparison of the results with the values of conventional light sources.

2 Theoretical background

2.1 Coherence of laser sources

One of the fundamental differences between laser radiation and radiation of conventional light sources is the degree of achievable spatial and temporal coherence. In this paper, we choose an approach of determining the temporal coherence length l_c of emitted light of two headlamp systems by using a Michelson interferometer.

A value for l_c that represents a border between laser radiation and radiation of conventional light sources does not exist. To get to know how much similarity the present radiation has to laser radiation, one can just compare the measured values with known data. Table 1 gives an overview for different light sources. An extensive literature research indicated that there do not exist values for light sources, which produce white light with the mechanism of phosphor conversion as the examined laser modules do.

Table 1: overview of l_c of different light sources [6–9, 19].

Light source	λ_0	$\Delta\lambda$	l_c
Sun (daylight)	550 nm	300 nm	900 nm
Light bulb	550 nm	300 nm	1 µm
LED	660 nm	25 nm	17 µm
Excimer laser KrF	248 nm	500 pm	40 µm
Excimer laser ArF	193 nm	320 pm	120 µm
Diode laser without stabilisation	n.a.	n.a.	<1 mm
Diode laser with stabilisation	760 nm	38 nm	15 mm
HeNe laser with stabilisation	6328 nm	1 fm	≤400 m

2.2 Static laser headlamp module

In the investigated laser headlamp, a static module is integrated to deliver additional high beam functionality at speeds above 60 km/h. A high-beam assistant depending on contraflow and preceding vehicles controls the laser spot [10]. Four blue laser diodes with a temperature-dependent typical emission wavelength of 450 nm are used, each delivering an optical output power of 1.6 W and a FHWM of less than 2 nm [11]. Collimation optics at the exit of the diodes collimate the radiation and, as depicted in Figure 1, a beam combining bundles it. The beam combining consists of two rhomboid prisms and a collecting lens [10, 2]. A subsequent light transmission bar homogenises the light, which is then redirected by a deflection mirror towards a phosphor converter [10]. The converter consists of a Yttrium aluminium garnet (YAG) crystal doped with Cerium [2]. In this transmissive configuration, a luminescence conversion of the blue radiation into spectral broadband light takes place with the help of conversion particles. The remaining blue radiation is scattered by scattering particles. The additive colour mixing of the scattered and converted light leads to white light [12]. A conclusive reflector produces the desired high-beam distribution. To prevent the emission of non-scattered radiation, a safety system on several levels is used [10].

2.3 Laser scanner prototype module

In contrast to the described static system, a laser scanner prototype and, thus, a dynamic arrangement were developed within the project “intelligent laser-based adaptive headlight system” (iLaS) [14]. A schematic overview of the components is depicted in Figure 2. The collimated beams

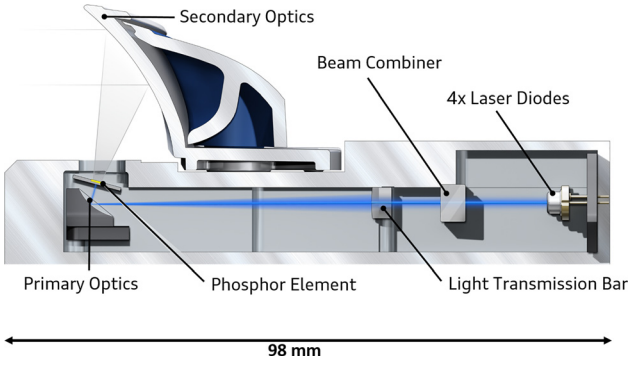

Figure 1: Schematic cut of a static laser module used in serial headlamps. From the study by Reich [13], modified.

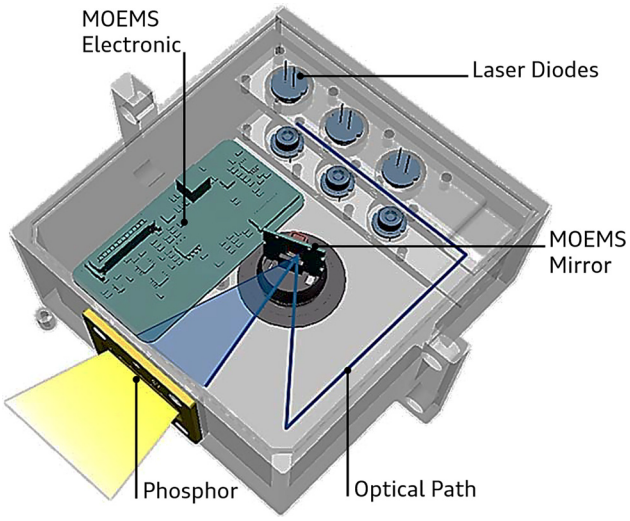

Figure 2: Schematic illustration of the functional principle of the laser scanner. From [17].

of six blue laser diodes with a typical wavelength of 447 nm and a total optical output power of 17 W hit a micro-optoelectro mechanical system (MOEMS) micro mirror. A different type of diodes than in the static module is used which also has a FHWM of less than 2 nm. The mirror deflects the six vertical aligned channels, while swivelling around the vertical rotating axis. Hence, the radiation is converted with the help of a transmissive phosphor converter as described above. A lens projects the resulting white light on the street. An observer perceives a constant impression of brightness due to the fast horizontal scanning. This is apparent in Figure 3, where the modulation of two laser channels due to the fast angular movement of the micro-mirror are shown [12–14].

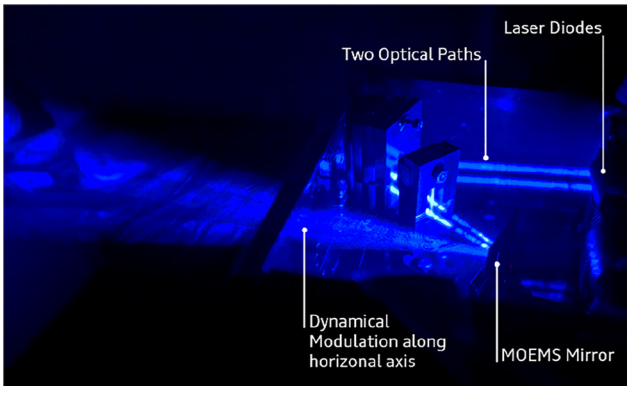

Figure 3: Open laser scanning module with two active laser channels. The phosphor is disassembled to show the optical path and modulation of the radiation. Modified, from [14].

The advantage of such a dynamic laser scanner system is the power neutral implementation of adaptive light distributions. A horizontal light centre positioning, a redistribution of light as well as a dynamic regulation of luminous intensity are made possible just through the adaption of the movements of the micro-mirror. In this way, opening angles between ±2° (motorway light at speeds above 160 km/h) and ±6° (standard high beam) can be realised. Since the total amount of light stays constant, smaller solid angles lead to higher maximum luminous intensities. Besides, de-glaring zones can be generated through an additional deactivation of individual laser diodes. Consequently, the light distribution can be adapted to the specific driving situation [12, 14–16].

3 Experimental setup

The Michelson interferometer kit EDU-MINT1/M of the company THORLABS was used. Initially, the mounting of the required components and their positioning and adjustment on the breadboard were carried out as described in [18] with a beam splitter BS, translational mirror M-t and rotational mirror M-r.

Due to the reflector design of the headlamp to illuminate the street optimally, an extended beam illuminates the experimental setup. To investigate only a narrow section of the light distribution with the maximum radiation, an adjustable iris diaphragm ID (Ø 0.7–8.0 mm) was positioned at one end of the breadboard. A selection of lenses with focal lengths f' of 50, 100 and 200 mm was provided to set the required divergence angle depending on the radiation angle of the examined headlamp. To ensure high flexibility and the optimal utilisation of the diameters of the components, enough space between the beam splitter and the diaphragm was given.

The adjusted interferometer was placed on a table in front of a goniophotometer (GPM) where the headlamp was mounted. The GPM was used to examine well-defined radiation directions and ensure the reproducibility of the setup. The table and the interferometer were adjusted in a way that the optical axis of the radiation emitted by the mounted headlamp hits the centre of the mirror M-t. As a starting point, the exit of the laser radiation was positioned in the intercept of the rotating axes of the GPM. The temporal coherence properties should be measured in the point of maximal irradiance because there exists the greatest potential danger. Therefore, a photodiode was positioned behind the iris diaphragm. The point of maximal output power was approximated iteratively

through translational and rotating movements. After the measurement position was found, a black cloth was fixed around the iris diaphragm and at the headlamp to prevent an overexposure of the interferometer. Subsequently, the diameter of the iris diaphragm was set. In principle, it should be as small as possible to avoid the influence of spatial coherence. Simultaneously, the interference pattern had to be illuminated homogeneously without shadowing effects and with a brightness which is comfortable to observe and which permits a clear detection of the interference effects. Besides, the divergence angle should not be too big to avoid overexposure and not too small to reach the largest possible pattern. Therefore, a compromise had to be found to reach all these goals while positioning one or two lenses at an optimal location between the diaphragm and the beam splitter. Figure 4 shows the resulting experimental setup.

Due to its responsivity which was variable for different wavelengths, the available photodiode was not able to record an interferogram by measuring the irradiance in the central circle of the ring pattern while moving M-t. It is to admit that the adjustment of the mirror M-t could not be done fine enough and the sensitivity of the interferometer and therefore the fluctuations of the interference pattern were too high to do so. Another possibility would have been the tilting of M-r in the white light position and taking a picture of the stripe pattern. Then a profile of the grey values could have been handled as an interferogram. However, this option was inhibited by the dimension of the present l_c because it exceeded an evaluable resolution of the pattern. Therefore, the measurement of l_c was carried out visually. This was done in the dark room after an adaptation time of 5 min to achieve the optimum possible outcome.

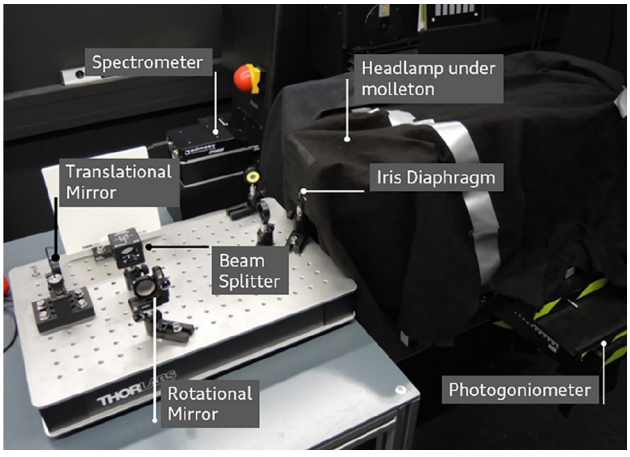

Figure 4: Resulting experimental setup.

Starting with a centred ring pattern from the white light position, the minimum of Visibility (V) was searched by moving M-t. The movement of the mirror was continued in the same direction for an additional distance of ca. 10 µm. Then, the direction was changed. While rotating the screw very slowly and stepwise, the minimum of Visibility was searched again, and the position of the micrometre screw was noted. By continuing the movement in this direction, the white light position was overrun, and the second minimum of Visibility was reached. The position of the screw was noted. The difference between the positions delivered an assessment for 0.5 l_c. The direction of the mirror movement was not allowed to change between the two minima, because of the mechanical play of the thread. The measurement was repeated four times; two times the screw was rotated in clockwise direction and two times counter clockwise to calculate the average and decrease the humanly source of error.

Finally, the spectrum of the evaluated radiation was measured to determine the relationship between l_c and the spectral characteristics. It was done by positioning the spectrometer behind the iris diaphragm. The maximum resolution of 0.5 nm was used. Another comparative measurement was done by moving the headlamp 60 mm sidewards to investigate the location dependency of the spectral properties. In each case, three measurements were averaged.

A further measurement was done using the headlamp including the static module. Additionally, a band pass interference filter with a transmission range of 415–455 nm was placed behind the iris diaphragm to isolate and evaluate the coherence properties of the initial laser radiation.

4 Results and discussion

The maximal irradiance was found by realising different rotations and translations. The headlamps were at close as possible next to the iris diaphragm because the divergence of the radiation induces a decreasing irradiance with increasing distance.

Referring to the static module a diameter of the iris diaphragm of 2.5 mm was combined with two lenses ($f_1' = f_2' = 50$ mm). A diameter of 5.0 mm combined with one lens with f' = 50 mm was adjusted to measure the laser scanner. As shown in Figure 6, for both headlamps, the resulting ring pattern was not exactly circular, because of the form of the light distribution.

The schematic course of the observed Visibility function V is depicted in Figure 5. It was a periodic one for both modules. Overall, five cycles could be clearly identified.

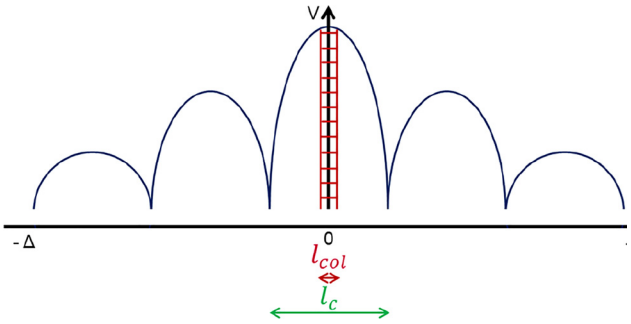

Figure 5: Schematic course of the Visibility function *V*, red hatched area: multi-coloured interference effects.

With increasing path difference (Δ), the maximal contrast of each cycle became worse. Outside of the cycles, the screen was illuminated with white light.

It existed just one area close to the white light position (red hatched region in Figure 5 with a length of l_{col}) in which colourful interference effects existed, whereby the colours became pale with rising Δ (Figure 6A and B). By exceeding l_{col}, a pattern of white and yellow rings (Figure 6C and D) remained. Its Visibility became worse until it reached a minimum. In this minimum, the contrast was not equal to 0 but very low. In accordance with the theoretical fundamentals of the measurement of temporal coherence and as shown in Figure 5, the range of Δ between the first minimums was measured to obtain l_c.

The occurrence of the observations can be explained by considering the spectrums of the two modules in the measurement position. The blue line in Figure 7 represents them. For a better comparison, the relative irradiances are plotted. Despite the spectrums of the modules were measured with different diameters of the diaphragm, they are comparable. This could be proven through comparative measurements, which indicated that the appearance of the spectrum does not change significantly by varying the diameter.

The spectrums consist of a peak, produced by the blue laser diodes, and a broadband part, which results from the conversion of the blue radiation into spectral broadband light. Due to scatter and conversion effects and the superimposition of several laser diodes, the peak is wider than the original spectrum of the used diodes. Deviations between the peak wavelength λ_{peak}, which was 444 nm for the static

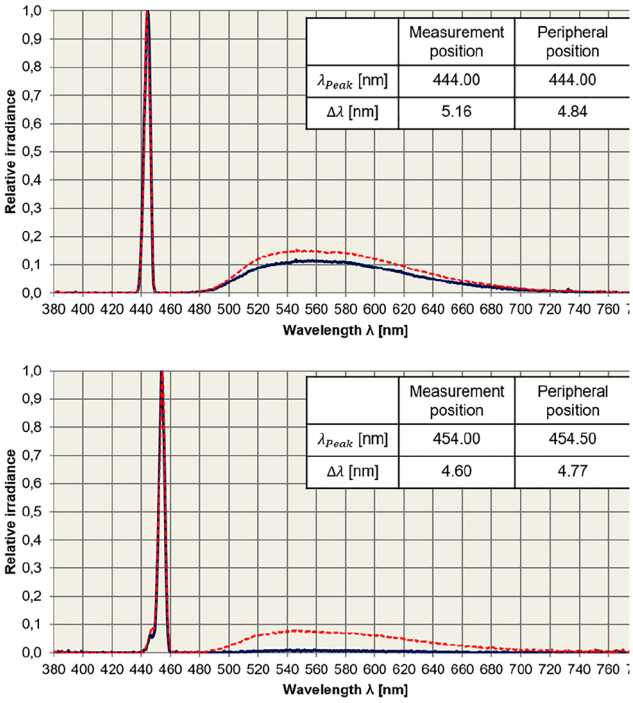

Figure 7: Spectrum of static headlamp module (top) and scanner module (below) including characteristic values; blue line: Measurement position, red line: peripheral position.

module and 454 nm for the scanner module, respectively, and the typical emission wavelengths of the used diodes can result from the temperature dependence of λ_{peak}. It can be seen that the spectral peak irradiance of the blue peak is about 10 times higher (static module) and 100 times higher (scanner module) than the irradiances of the wavelengths within the broadband part. Close to the white light position, colourful interference effects could be observed due to the short coherent broadband part. The effects outside of the white light position area resulted from the narrowband blue peak, which led to an interference pattern that showed blue rings in the case of constructive interference and dark rings in the case of destructive interference. The periodic course of the Visibility function with decreasing maximums of *V* was probably reached because of the mode structure of the individual lasers and their superimposition. The fact that the contrast of the minima was not equal to 0 indicates that the spectral components of the laser radiation had different irradiances. However, the blue pattern could not be detected,

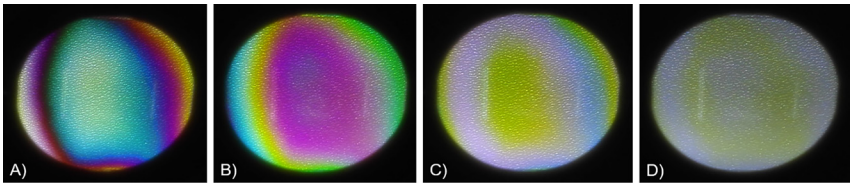

Figure 6: Ring patterns depending on the present Δ. From A) to D): growing Δ; A) Close to white light position; D) Close to minimum of contrast.

because of the overlap of the broadband radiation. Therefore, white rings resulted in the event of constructive interference of the blue light because the mixture of all wavelengths which occur in the spectrum leads to white light. In the event of destructive interference of the blue radiation, yellow rings could be detected because white light minus the blue part leads to a yellow colour impression. Due to the high relative irradiance of the blue peak, the pattern of yellow and white rings could be clearly observed. With increasing Δ, the decreasing contrast of the blue pattern led to a decreasing Visibility of the yellow-white pattern. Outside of the five cycles, the irradiance and the contrast of the blue pattern were not high enough to lead to the white-yellow interference effects any more.

The measured values for l_c and l_{col} are listed in Table 2. The arithmetic average of l_{col} was 9.8 µm for the static module and 8.0 µm for the scanner module, whereby the greater value of the static module can be explained by the more pronounced spectral broadband part of the spectrum.

On the contrary, l_c of the scanner module was 147.0 µm and l_c of the static module was less with just 92.5 µm. In accordance with this, the total range of Δ in which interference effects could be observed was larger for the scanner module. The mode structure of the individual lasers, their superimposition, and the interacting with the phosphor converter lead to the observed appearance of the blue peak, which determines the coherence properties of the radiation. Differences between the two modules can have several causes like the use of diodes from a different type with their diverse mode structure, different phosphor converters, and the varying functional principle. A $\Delta\lambda$ of 5.16 and 4.60 nm was observed for the static and scanner module, respectively. This coincides with the theoretical background, where the temporal coherence gets worse with increasing $\Delta\lambda$. But the measured values deviate from the theoretic ones of 38.2 µm for the static module and 44.8 µm for the scanner module which were calculated by the quotient of $\lambda_0^2/\Delta\lambda$. In place of the central wavelength of the total spectrum, λ_{peak}, which is nearly the same as the central wavelength of the peak, was used to simplify the calculation. This was done because as described above, the appearance of the blue peak was primarily responsible for the measured l_c. Reasons for the deviation could include the specific shape of the present peak and the non-consideration of the mode structure through the equations.

Table 2: overview of the measured coherence lengths.

Direction of measurement	Static module			Laser scanner module	
	Without filter		With filter		
	l_c (µm)	l_{col} (µm)	l_c (µm)	l_c (µm)	l_{col} (µm)
Clockwise	92.0	9.0	95.0	145.0	8.0
Clockwise	94.0	10.0	93.0	150.0	8.0
Counterclockwise	90.0	10.0	91.0	147.0	8.0
Counterclockwise	94.0	10.0	92.0	146.0	8.0
Average	92.5	9.8	92.8	147.0	8.0

Figure 7 also includes a comparison between the spectrum existing in the measurement position and the spectrum of the peripheral position (red line). Both modules show a local dependency of the spectrum and $\Delta\lambda$. The spectrum of the scanner module shows that almost no converted light existed in the position of maximal irradiance. Reasons for the observed variability could include that the scattering and conversion effects depend on the particular direction of the radiation. The different phosphor converters and functional principles could cause differences between the two modules. The local dependency indicates that also the temporal coherence properties vary with different measuring points. Therefore, further investigations of l_c as a function of different positions relative to the headlamp should be realised.

To further investigate the described explanation of the observations concerning the significance of the blue peak for the appearance of the ring pattern and the temporal coherence properties, another measurement of the static module with an additional band pass filter was done. The diameter of the iris diaphragm had to be increased to 3.5 mm to reach a sufficient irradiance on the screen. The position of the headlamp was identical to the previous measurement. A spectral measurement assured the desired function of the filter; just the unchanged blue peak was transmitted through it. The observations accorded with the explanations above. A ring pattern of blue and dark rings as shown in Figure 8 was visible on the screen.

By removing the filter, it became evident that the constructive interference of the blue radiation led to white rings and the destructive interference to yellow rings. The Visibility function had the same course as described above (compare Figure 8A–C), but more than five periods could be observed because the superposition of the broadband spectral part was eliminated. Thus, interference effects could be detected in a range of Δ of 1600 µm in comparison to 600 µm without filter. Consequently, the measured l_c of 92.8 µm (Table 2) was almost identical to the primary measurement. These results show, that the measured values for l_c caused by the blue peak of the spectrum.

It has to be considered that the visual evaluation of the interference effects was not as accurate as the evaluation of

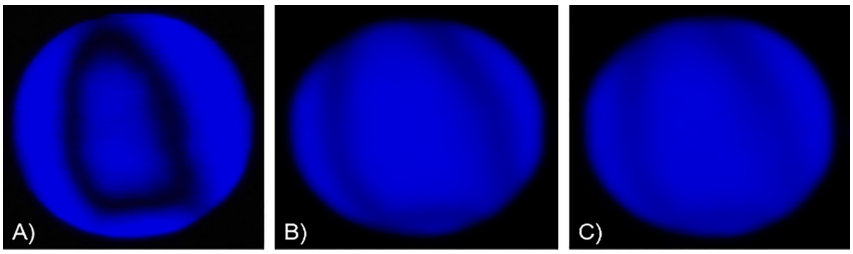

Figure 8: Ring patterns observable with band pass filter depending on the present Δ, from A) to C): Growing Δ; A) Close to white light position; C) Close to minimum of contrast.

a recorded interferogram would have been. The determination of the minimums of the Visibility function was subjective and difficult because the contrast was not equal to 0 in these points. For follow-up measurements, it would be useful to use a combination of a piezoelectric crystal which can realise movements of the mirror M-t in a nanometre range and a detector that provides a wavelength independent responsivity in the visible spectral range. Through the coupling of the tools, the precise evaluation of a recorded interferogram would be possible. Another uncertainty of measurement was given because the ring pattern was not exactly centric within the total range of the mirror movement. This resulted from slight deviations concerning the adjustment of the interferometer. Nevertheless, the observations provide a good indication for the temporal coherence properties of the radiation emitted by the laser modules. The measured spectrums, the periodic course of the Visibility function, and the dimension of the measured values for l_c show that the radiation seems to have in part properties of laser radiation. Hence, the evaluated laser modules of the headlamps cannot be considered as conventional white light sources completely. Indeed, the results illustrate that they can rather be seen as radiation sources which provide narrowband coherent blue laser-like radiation originating from the laser diodes and broadband incoherent light originating from the conversion, whereby the two parts are superimposed. Therefore, the measured values of l_{col} can approximately be treated as the coherence length for the broadband portion and the values of l_c for the narrowband part. In comparison with Table 1, the obtained values for l_{col} are in the region of daylight of the sun and a light bulb. The values for l_c are significantly greater than the values for the light bulb and therefore, they can rather be allocated to the region of a diode laser without stabilisation. When comparing the measured coherence lengths to the typical values in Table 1, it must be kept in mind that no consistent definition on which value the Visibility function must be decreased to obtain the coherence length exists. Besides, it is not known whether the reference coherence lengths of laser diodes were determined by the minimums of the Visibility function or the total range in which interference effects could be observed. Consequently, the reference values can just be considered as a rough indicator for the dimension of the coherence length.

To adapt the coherence properties of the laser modules to a white light source, the spectrums have to be attuned to the ones of a white light source. The spectrum of a white LED could serve as a model. This seems to be obvious because white LEDs used in headlamps are also based on a luminescence conversion of blue radiation into spectral broadband light. Therefore, this spectrum should be the easiest to achieve. An example is shown in Figure 9. In addition, the comparison with the LED offers the advantage that the coherence properties of a LED headlight could be measured with the same procedure and criteria as used for the laser module. In this way, the reliance on reference values whose occurrence is not known would be eliminated.

Initially, l_c of a laser module without phosphor converter should be determined to find out which degradation of the coherence properties in comparison to the initial laser radiation could be achieved through the scattering and conversion of the phosphor converter. This would also be insightful to clarify the reasons for the periodicity of the Visibility function. With the help of this knowledge, the blue laser peak and the broadband part have to be

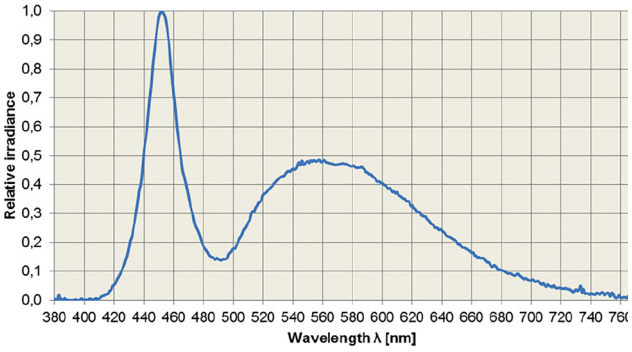

Figure 9: Example of a spectrum of a white LED based on luminescence conversion.

broadened to achieve their merging. When the mode structure is the decisive reason for the periodicity, an elimination of it would be helpful. For one thing, a mode structure is a typical property of laser radiation, on the other hand, its influence makes the relation between spectrum and coherence properties even more complicated. Besides, more power of the initial laser radiation has to be converted into broadband light. Since the line broadening based on scattering effects is not sufficient to reach these goals, an extensive modification of the phosphor converter seems necessary. A permanent control of the coherence properties with the interferometer during this iterative process of changing the spectrum is required but also time consuming. To reduce the measuring effort, it should be examined if the evaluation of an interferogram obtained with the help of a Fourier transformation of the measured spectrum delivers the same result for the coherence length. In addition, the polarisation of the initial laser radiation, of the blue peak after the interaction with the phosphor converter, and of the converted broadband radiation should be evaluated to find out whether polarisation effects had an influence on the results.

5 Summary and conclusion

Difficulties concerning the field of classification for laser products which work in conventional headlamps were the motivation for the investigation of the temporal coherence properties of two different laser modules used in headlights. For this purpose, an experimental setup including a goniophotometer, which allowed the examination of well-defined radiation directions, a spectrometer to analyse the connection between the spectral characteristics and the coherence properties, and a Michelson interferometer was built up. Measurements were performed in the point of maximal irradiance and evaluated visually. The results indicated that the laser modules of the headlights could be considered as light sources that emit narrowband coherent blue laser-like radiation originating from the laser diodes and broadband incoherent light originating from the conversion, whereby the two parts are superimposed. Several indicators as the appearance of the measured spectrums, the periodic course of the Visibility functions, and the dimension of the measured coherence lengths led to this conclusion. This was confirmed by an additional measurement using a band pass interference filter transmitting just the blue light. A coherence length of 9.8 and 8.0 µm could be measured for the broadband part of the static and the scanner module, respectively. For the narrowband portion, coherence lengths of 92.5 and 147.0 µm were determined. Therefore, the emitted radiation of laser modules has in part properties of laser radiation, and the laser headlamps cannot be considered as conventional white light sources completely. Further investigations including measurements of the laser modules without phosphor converter, the record of interferograms and their Fourier transformation, the evaluation of the influence of polarization effects, and location-dependent measurements of the coherence properties should be performed. Prospective measurements of the coherence length should be done by integrating a piezoelectric crystal and a suitable detector into the interferometer to increase the measurement accuracy. The adjustment of the spectrum to the spectral characteristics of a white LED based on luminescence conversion appears appropriate to eliminate the similarities to laser radiation.

Author contribution: All the authors have accepted responsibility for the entire content of this submitted manuscript and approved submission.
Research funding: None declared.
Conflict of interest statement: The authors declare no conflicts of interest regarding this article.

References

[1] J. Wilhelmy and C. Gut, "Laser headlamps: key factors and improvement," in *ISAL 2015 – 11th International Symposium on Automotive Lighting*, T. Q. Khanh, Ed., München, Herbert Utz Verlag GmbH, 2015, pp. 405–414.
[2] C. Gut, V. Krstajic, and S. Berlitz, "Laserscheinwerfer: Vom Motorsport zur Serie," *Elektronik Automotive*, no. 10, pp. 44–48, 2014.
[3] K. Schulmeister and J. Daem, "Classification of laser illuminated light sources under IEC 60825-1 Edition 3," in *Proceeding of the International Laser Safety Conference. March 20-23, 2017 Atlanta, GA USA*, Laser Institute of America, Ed., 2017, pp. 174–180.
[4] DIN Deutsches Institut für Normung e. V. and VDE Verband der Elektrotechnik Elektronik Informationstechnik e. V. DIN EN 62471, Photobiologische Sicherheit von Lampen und Lampensystemen .
[5] IEC International Electrotechnical Commission. IEC 60825-1 Edition 3.0, Safety of laser products – Part 1: Equipment classification and requirements .
[6] H.-J. Eichler and J. Eichler, *Laser. Bauformen, Strahlführung, Anwendungen. 8., aktualisierte und überarb. Aufl*, Berlin, Springer Vieweg, 2015, Lehrbuch. ISBN 9783642414374.
[7] E. Hecht, *Optik. 5., verbesserte Auflage*, München, Oldenbourg Wissenschaftsverlag GmbH, 2009, ISBN 9783486588613.
[8] T. Pflanz and H. Huber, "The compact excimer laser -lightsource for optical (mask)inspection systems," in *Proceedings of SPIE – The International Society for Optical Engineering*, vol. 4349, 2001.

[9] G. Litfin, *Technische Optik in der Praxis. 3., aktual. und erw. Aufl*, Berlin, Springer, 2005, ISBN 354021884x.
[10] A. Mittenhuber, *Aufbau und Inbetriebnahme eines Prüfstandes für Lasermodule von Kraftfahrzeugscheinwerfern*, Bachelor thesis, Kempten, 2017.
[11] OSRAM OPTO SEMICONDUCTORS GMBH, *Blue Laser Diode in TO56 Package. Version 0.3*, Regensburg, 17, 2015.
[12] A. Petersen, J. Hager, C. Gut, et al., "Challenges for MEMS based scanning laser system," in *ISAL 2015 – 11th International Symposium on Automotive Lighting*, T. Q. Khanh, Ed., München, Herbert Utz Verlag GmbH, 2015, pp. 355–364.
[13] S. Reich, *Entwicklung LASER Scheinwerfer. Konstruktive Besonderheiten*, Ingolstadt, 30, 2014.
[14] J. Hager, M. Seitz, C. Bemmer, et al., *Handling 17 W of Scanning Laser Power – Three Years of Exploration in the iLaS Project*, ISAL, 2017.
[15] M. Fischer, *Homogenitätsbewertung eines dynamischen Laserscheinwerfer-Systems*, Master thesis. Aalen, 29, 2017.
[16] C. Gut, A. Petersen, P. Jahn, M. Seitz, C. Neumann, and S. Berlitz, "Das ideale Licht: Mikromechanischer Matrix laser Scheinwerfer," in *ELIV – Kongress zur Fahrzeugelektronik*, VDI WISSENSFORUM GMBH, Ed., Düsseldorf: VDI Verlag, 2015, pp. 277–292.
[17] Internal document within the scope of the govermental founded research project iLaS .
[18] THORLABS, *Michelson-Interferometer Kit Handbuch*, 2016.
[19] H. Naumann, G. Schröder, and M. Löffler-Mang, *Handbuch Bauelemente der Optik. Grundlagen, Werkstoffe, Geräte, Messtechnik. 7., vollständig überarbeitete und erweiterte Aufl*, München, Hanser, 2014, ISBN 978-3446426252.

Bionotes

Valerie Popp
Entwicklung Innovationen Licht/Sicht, AUDI AG, Ingolstadt, Germany
valerie.graf@gmail.com

Valerie Popp studied Ophthalmic Optics/Optometry and Laser- and Optotechnologies at the University of Applied Sciences of Jena, Germany. During a student internship in the Development Innovations Light/Visibility department at Audi in Ingolstadt, Germany, she investigated the temporal coherence properties of laser modules used in headlamps. She wrote her master's thesis in the field of refractive laser surgery at Technolas Perfect Vision in Munich, Germany. At the moment, she is on parental leave.

Philipp Ansorg
Entwicklung Funktionen Licht, AUDI AG, Ingolstadt, Germany
philipp.ansorg@audi.de

Philipp Ansorg studied Physics at the University of Göttingen, Germany. Afterwards he worked on his PhD at Audi and the Light Technology Institute at the Karlsruhe Institute of Technology, Germany. His research focuses on laser based headlamp systems. Since 2018 he works in the Light functions development department at Audi in Ingolstadt, Germany.

Burkhard Fleck
SciTec – Präzision-Optik-Materialien, Ernst-Abbe-Hochschule Jena, Jena, Germany
burkhard.fleck@eah-jena.de

Burkhard Fleck studied Physics at the University of Jena. After completing his PhD, he worked in the field of coherent optical measurement technology. He habilitated in 2000 at the Faculty of Physics and Astronomy at the University of Jena. In 2001 he became professor for Technical Optics and Physics at the Ernst Abbe University (University of Applied Sciences) in Jena.

Cornelius Neumann
Lichttechnisches Institut, Karlsruher Institut für Technologie, Karlsruhe, Germany
cornelius.neumann@kit.edu

Cornelius Neumann studied Physics and Philosophy at the University of Bielefeld, Germany. After his PhD, he worked for the automotive supplier Hella in the advanced development for Automotive Lighting. During his time at Hella he was responsible for signal lighting, LED application and acted as a director of the L-LAB, a laboratory for lighting and mechatronics in public private partnership with the University of Paderborn, Germany. In 2009, he became Professor for Optical Technologies in Automotive and General Lighting and one of the two directors of the Light Technology Institute at the Karlsruhe Institute of Technology, Germany.